EUROPEAN ORGANISATION FOR NUCLEAR RESEARCH

OPAL physics note PN 183
eps-290
17-July-1995

A Measurement of the Charm and Bottom Forward Backward Asymmetry using D Mesons with the OPAL Detector at LEP

Abstract

A measurement of the charm and bottom forward backward asymmetry is presented at energies on and around the peak of the Z^0 resonance. Charm and bottom decays are identified using decays of D mesons in about 3.5 million hadronic decays of the Z^0 boson recorded with the OPAL detector at LEP between 1990 and 1994. Using seven different decay modes approximately 27000 D mesons are tagged. From these the charm and bottom asymmetries are measured in three energy ranges around the Z^0 peak:

$A^c_{FB} = -0.006 \pm 0.068 \pm 0.012 \quad A^b_{FB} = 0.027 \pm 0.169 \pm 0.039 \quad \langle E_{cm} \rangle = 89.54$ GeV
$A^c_{FB} = 0.068 \pm 0.014 \pm 0.007 \quad A^b_{FB} = 0.112 \pm 0.035 \pm 0.021 \quad \langle E_{cm} \rangle = 91.20$ GeV
$A^c_{FB} = 0.171 \pm 0.058 \pm 0.015 \quad A^b_{FB} = -0.267 \pm 0.140 \pm 0.050 \quad \langle E_{cm} \rangle = 92.94$ GeV

in agreement with the predictions of the standard model and other measurements at LEP.

This note describes preliminary OPAL results submitted to the EPS conference, Brussels, July 1995, and the Lepton-Photon Conference, Beijing, August 1995.

1 Introduction

Electroweak measurement involving heavy quarks have become a subject of extensive study at LEP in recent years [1]. An important goal of these experiments is the precise measurement of the coupling constants of the weak currents and their comparison with the predictions of the standard model. The angular distribution of the final state fermions provides a probe of these coupling constants. The different strengths of the left handed and the right handed components of the neutral weak current result in an asymmetry of the differential production cross section relative to the direction of the initial state fermion. In addition the electromagnetic and the neutral weak currents interfere. On the peak of the Z^0 resonance this latter interference vanishes to first order, but it becomes more and more important at energies away from the Z^0 pole. In the standard model, to lowest order, for centre-of-mass energies close to the Z^0 mass, the distribution in $\cos\theta$ [1] can be written:

$$\frac{\mathrm{d}\sigma}{\mathrm{d}\cos\theta} \propto 1 + \cos^2\theta + \frac{8}{3} A_{\mathrm{FB}}^{\mathrm{f}} \cos\theta \ . \tag{1}$$

On the pole of the Z^0 resonance for quark flavour Q, $A_{\mathrm{FB}}^{\mathrm{Q},0}$, the forward-backward asymmetry, can be expressed as

$$A_{\mathrm{FB}}^{\mathrm{Q},0} = \frac{3}{4} \mathcal{A}_{\mathrm{e}} \mathcal{A}_{\mathrm{Q}} \ , \tag{2}$$

where $\mathcal{A}_{\mathrm{e}}$ and $\mathcal{A}_{\mathrm{Q}}$ are a function of the electroweak coupling constants $g_{\mathrm{V}}^{\mathrm{f}}$ and $g_{\mathrm{A}}^{\mathrm{f}}$:

$$\mathcal{A}_{\mathrm{f}} = \frac{2 g_{\mathrm{V}}^{\mathrm{f}} g_{\mathrm{A}}^{\mathrm{f}}}{(g_{\mathrm{V}}^{\mathrm{f}})^2 + (g_{\mathrm{A}}^{\mathrm{f}})^2} \ . \tag{3}$$

In this paper measurements of the forward-backward asymmetries in the processes $e^+e^- \to c\overline{c}$ and $e^+e^- \to b\overline{b}$ are presented. Charm and bottom events are tagged using $D^{*\pm}$, D^0 and $D^{\pm}$ mesons in a number of different decay modes. The flavour composition of the tagged sample is determined on a statistical basis based upon lifetime information and the specific topologies of bottom jets compared to other jets. The forward-backward asymmetry of charm and bottom quarks is fitted using an unbinned maximum likelihood fit. The separation between the main contributions to the signal is improved by including weights calculated individually for each event based upon lifetime information. The measurement presented is an extension and an update to the one published in [2].

The paper is structured as follows. After a presentation of the techniques used to reconstruct the different D states, the method used in determining the flavour composition is discussed. These sections rely on work previously published by OPAL [2,3]. The results from this analysis, the fractions of D mesons that are charm and bottom events, are used as input in the fit to the thrust direction distribution, signed by the charge of the identified candidate[2]. Particular emphasis is placed on the method in which lifetime information is used to improve the fit for the charm and bottom asymmetries. The fit is performed for three energy ranges spanning approximately $M_{\mathrm{Z}^0} - 3$ GeV to $M_{\mathrm{Z}^0} + 3$ GeV.

[1] Here $\cos\theta$ denotes the angle between the incoming and the outgoing fermion in the process $e^+e^- \to q\overline{q}$.

[2] The charge of the D candidates is defined by the charge of the charm quark in the quark model for this D meson

2 OPAL Detector

A complete description of the OPAL detector can be found in references [5]. Only the components relevant for the analysis presented are summarised. Tracking of charged particles is performed in a central detector, consisting of (going from the beampipe outwards) two layers of silicon micro vertex detectors, a high precision vertex drift chamber, a large volume jet chamber, and a set of drift chambers which measure the coordinates of tracks along the direction of the beam line (z-chambers). The central detector is contained inside a solenoidal magnet producing a homogeneous field of 0.435 T. High precision reconstruction of secondary vertices is possible using the silicon micro vertex detector, which covers polar angles $|\cos\theta| < 0.83$ with at least one layer of silicon detectors, or $|\cos\theta| < 0.77$ with two layers. Tracking using the combined detectors is possible over nearly the full solid angle down to $|\cos\theta| < 0.98$.

The magnet coil is surrounded by a time-of-flight scintillator counter array and a lead glass electro-magnetic calorimeter. A presampler is installed between these components which allows an improvement of the measurement of the longitudinal shower development and spatial resolution for showers having started in the magnet coil of the detector, and provides an additional space point on tracks leaving the central tracking system. The magnet return yoke is instrumented with nine layers of limited streamer tubes and serves as a hadronic calorimeter. Outside the hadron calorimeter 93% of the solid angle is covered by at least 2 layers of muon chambers.

Particle identification for charged particles is performed using the specific energy loss, $\mathrm{d}E/\mathrm{d}x$, in the jet chamber. Electrons and muons are identified in addition with the help of information from the calorimeters and muon chambers.

3 Hadronic Event Selection and Simulation

Hadronic Z^0 decays are selected based upon requirements on the number of charged tracks reconstructed and the energy deposited in the calorimeter. A detailed description of the criteria is given in ref. [6]. Charged tracks and electromagnetic clusters unassociated with tracks are grouped into jets using the JADE jet finder and the E0 recombination scheme [7] with a cutoff value of $x_{min} = 49$ GeV^2. The primary vertex in a collision is reconstructed from the charged tracks in the event and constrained in addition with the known average beam position and spread of the e^+e^- collision point.

The analysis is based on about 3.5 million hadronic decays of the Z^0 collected with the OPAL detector in the vicinity of the Z^0 pole between 1990 and 1994. Of these data roughly 10% have been collected either below or above the maximum of the resonance.

To check procedures and investigate possible biases, 2.5 million hadronic decays of the Z^0 have been simulated using the JETSET Monte Carlo model [8] with parameters tuned to represent well LEP data [9]. A number of special samples have been used to study specific decays, which correspond to an additional 5 million hadronic Z^0 decays. In all samples heavy quark fragmentation has been modeled using the model of Peterson *et al.* [10]. All samples were passed through a detailed simulation of the OPAL detector [12] before being analysed using the same programs as for data.

4 Selection of D Candidates

Three different D meson states are used in this paper as tags for charm and bottom: the ground state D mesons D^0 and D^+ [3], and the spin 1 state D^{*+}. After describing the requirements placed on tracks to be used in the analysis, the reconstruction and the requirements used in the identification of charged D^* mesons are discussed, followed by the same discussion for D^0 and D^+ mesons. Additional details on D reconstruction with the OPAL detector can be found in [2–4].

Tracks are used in the reconstruction if they satisfy the following track quality requirements:

- $|d_0| < 5$ mm;
- $|z_0| < 20$ cm;
- $p_t > 250$ MeV;
- $n_{CJ} > 40$.

Here d_0 is the distance of closest approach between the primary vertex and the track measured in the plane perpendicular to the beam, z_0 is the distance along the beam at this point, p_t is the momentum component perpendicular to the beam, and n_{CJ} is the number of hits on the track recorded in the central drift chamber. To reject poorly reconstructed tracks a good z measurement is required by selecting only tracks which have either hits in the z-chambers, an associated endpoint hit[4] or have been merged to a cluster found in the barrel presampler.

4.1 D^{*+} Reconstruction

For this analysis D^{*+}mesons are reconstructed in five different decay channels:

$$
\begin{array}{lll}
D^{*+} \to D^0\pi^+ & & \\
\quad \hookrightarrow K^-\pi^+ & \text{“3 prong”} & , \\
\quad \hookrightarrow K^-\pi^+\pi^0 & \text{“satellite”} & , \\
\quad \hookrightarrow K^-\pi^+\pi^-\pi^+ & \text{“5 prong”} & , \\
\quad \hookrightarrow K^-e^+\nu_e & \text{“electron”} & , \\
\quad \hookrightarrow K^-\mu^+\nu_\mu & \text{“muon”} & .
\end{array}
$$

No attempt is made to reconstruct the π^0 in the satellite channel, nor the neutrino direction or energy in the electron and muon channels. The last two channels are referred to as “semileptonic” channels in the following. Electrons are identified based on the energy loss in the central drift chamber and the energy deposition in the electromagnetic calorimeter. An artificial neural network trained using simulated events is used to perform the selection [13]. Electrons from conversions are rejected as in [14]. Muon candidates are identified by associating tracks found

[3] Throughout this paper charge conjugate modes are always implicitly included.

[4] The endpoint method is used for tracks leaving the central detector with $|\cos\theta| > 0.7$ to improve the polar-angle measurement. It uses the knowledge of the end position of the last wire in the jet-chamber which registered a hit to derive a z coordinate measurement.

in the central tracking system with tracks in the outer muon chambers [14]. No momentum cut is applied since the knowledge of the lepton purity is not required in the subsequent analysis.

A number of tracks appropriate for the selected channel are combined to form a candidate for a D^0, and its invariant mass is calculated. Only candidates with the correct charge combinations are used. Candidates are selected if the reconstructed mass lies within the expected range. After adding a further track as a candidate for the pion in the D^{*+} decay the combined mass is calculated and the candidate is selected if the mass difference $\Delta M = M_{D^{*+}} - M_{D^0}$ is within given limits. Note that ΔM for channels with missing decay partners is to be understood as the effective mass difference, calculated only from the visible tracks of the candidate. This latter requirement is particularly efficient in suppressing background, because the small mass difference between the D^{*+} and the D^0 places true D^{*+} decays very close to the kinematic threshold in ΔM at 0.139 GeV. Very little phase space remains for background events, resulting in a good signal to background ratio.

At low $x_{D^{*+}} = E^{calc}_{D^{*+}}/E_{beam}$ [5] background especially from pions produced in the fragmentation is very high. The particle identification power of the OPAL detector is used to enrich the sample in true kaons. For a kaon candidate requirements are placed on the probability $W^{KK}_{dE/dx}$, that the dE/dx measurement of this track was produced by a kaon.

Background to the sample is further reduced by cutting on the helicity angle θ^*, measured between the direction of the D^0 candidate in the laboratory frame and the direction of the kaon in the rest frame of the D^0 candidate. True D^0 decays are expected to be isotropically distributed in the quantity, while background displays pronounced peaks at $\cos\theta^* = -1$ and, particularly at low $x_{D^{*+}}$, $\cos\theta^* = +1$.

The analysis is done separately for three classes of candidates:

- z-chamber candidates: All tracks of the candidates have a hit in the z chamber.
- endpoint candidates: At least one track has an endpoint measurement.
- presampler candidate: At least one track has a presampler measurement.

A detailed list of the cuts is given in table 1.

4.2 D^0 and D^+ Reconstruction

The D^0 and D^+ mesons are identified in the following decay modes:

$$D^0 \to K^-\pi^+ \ ,$$
$$D^+ \to K^-\pi^+\pi^+ \ .$$

The reconstruction of these D meson states proceeds similar as for the D^{*+} mesons. The invariant mass is calculated from the appropriate number of tracks which passed the quality requirements. A D^+ candidate is rejected if the mass difference ΔM, calculated under the

[5] In this paper any reference to the scaled energy x of a D candidate is to be understood as being to the calculated scaled energy, obtained from the reconstructed tracks, without correcting for missing or wrongly associated tracks.

cut	x-range	3 pr	semil.	sat.	5 pr.
$x_{\mathrm{D}^{*+}}$		$0.2 - 1.0$	$0.2 - 1.0$	$0.2 - 1.0$	$0.5 - 1.0$
M_{D^0} [GeV]	full	$1.79 - 1.94$	$1.20 - 1.80$	$1.41 - 1.77$	$1.79 - 1.94$
ΔM [GeV]	full	$0.142 - 0.149$	$0.140 - 0.162$	$0.141 - 0.152$	$0.142 - 0.149$
$\cos\theta^*$	< 0.5	$-0.8 - 0.8$			-
	> 0.5	$-0.9 - 1.0$			$-0.9 - 1.0$
$\lvert W^{\mathrm{KK}}_{\mathrm{d}E/dx}\rvert$	< 0.5	> 0.1			-

Table 1: List of cuts used in the D^{*+} reconstructions. Note that both the scaled energy x_{D} and the mass difference ΔM are effective quantities, calculated from the reconstructed tracks only. The exact meaning of the different quantities is explained in the text.

assumption that the three tracks form a D^{*+} candidate, is below 0.16GeV. To suppress combinatorial background, and to allow a good measurement of the specific energy loss $\mathrm{d}E/dx$, candidates are required to have at least 30% of the beam energy, and the individual track momenta are to be above 1.5 GeVfor a kaon, 0.5 GeVfor a pion. The long lifetime of the weakly decaying D mesons is used to enrich the signal purity. A vertex is calculated from the intersection of the tracks forming the D candidate in the $r - \phi$ plane. The distance d between this vertex and the primary event vertex is calculated. A candidate is accepted if this distance exceeds some length. Good quality of the vertex reconstruction is ensured by requiring that at least one (for the D^0) or two (for the D^+) tracks have at least one hit in the silicon micro vertex detector. To stay within the acceptance of this detector, all tracks have to be within $|\cos\theta| < 0.85$. For the D^+, where three tracks in the decay allow a sensible calculation of a vertex χ^2, this has to be less than 25 to be accepted.

The number of multiple candidates and wrong particle type associations is reduced by placing requirements on the $\mathrm{d}E/dx$ measurement. Kaon candidate tracks are required to be consistent with being a kaon with a probability $W^{\mathrm{KK}}_{\mathrm{d}E/dx}$ exceeding 3%, if their measured $\mathrm{d}E/dx$ is above the value expected for a kaon, and exceeding 1%, if the measured $\mathrm{d}E/dx$ is below the expected value. Pion background is rejected by accepting only tracks whose probability $W^{\mathrm{K}\pi}_{\mathrm{d}E/dx}$ that the track be consistent with a pion is less than 10%.

The analysis is repeated for the three classes of events (z-chamber candidates, endpoint candidates and presampler candidates) present in the sample. The details of the cuts are listed in table 2.

4.3 Multiple Candidate Rejection

Since the goal of the analysis is the determination of the angular distribution of the primary quark, not that of reconstructed mesons, only one measurement of this quantity per event is needed. If more than one candidate meson is found per event, a hierarchy is used to select the best one: low background is preferred and low multiplicity final states over higher multiplicity ones. The hierarchy used is: 3-prong > semileptonic > satellite > 5-prong > D^0 > D^+. If more than one candidate is found within one D^{*+} channel, the one with the D^0 mass closest to the nominal mass is taken (the mass used is 1.865 GeV for the 3-prong, semileptonic and 5-prong decay, and 1.60 GeV for the satellite). In the D^0 and D^+ decays, where a selection on the mass

cut	D^0	D^+
x_D	$0.3 - 1.0$	$0.3 - 1.0$
M_{D^0,D^+}[GeV]	$1.81 - 1.93$	$1.81 - 1.93$
ΔM[GeV]	-	> 0.16
p_K[GeV]	> 1.5	> 1.5
p_π[GeV]	> 0.5	> 0.5
$\lvert cos\theta_{cand}\rvert$	< 0.85	< 0.85
$d[\mu m]$	> 500	> 800
$W^{KK}_{dE/dx}$	> 0.03	> 0.03
	< -0.01	< -0.01
$\lvert W^{\pi\pi}_{dE/dx}\rvert$	> 0.01	> 0.01
$\lvert W^{K\pi}_{dE/dx}\rvert$	< 0.1	< 0.1

Table 2: List of cuts used in the D^0 and D^+ reconstruction. The exact meaning of the different quantities is explained in the text.

	lost in total [%]	within channel [%]
3-prong	9.2	9.2
semileptonic	17.9	12.5
satellite	29.6	21.0
5-prong	58.6	55.2
D^0	39.8	33.3
D^+	55.6	52.6

Table 3: Percentage of candidates lost in the multiple candidate rejection. Given for each channel are the total percentage of candidates rejected, and the percentage of candidates rejected only due to multiple candidates found within this channel.

would result in a distortion of the invariant mass spectrum, the candidate with the highest x_D is selected. In table 3 the percentage of events rejected due to this procedure in each channel is shown. After all cuts a total of 60277 candidates are found.

4.4 Background to D^0, D^+ and D^{*+}

Backgrounds to the different channels come from a number of different sources. The majority of background candidates are random combinations of tracks ("combinatorial background"), which do not originate from a common parent, but pass the applied cuts. They are heavily concentrated at low x_D. Partial reconstructions of other heavy meson decays, in particular other D meson decay modes, form another important contribution. They are of particular relevance in the D^{*+} channels, because even if only some of the D^0 decay products are correctly identified, these events still show the characteristic enhancement in ΔM around 145 MeV, if the slow pion is correctly identified. In addition a correctly identified slow pion implies that the charge of the candidate is related to the charge of the primary quark in the same way as

is the case for a true D^{*+} meson. Such events can therefore be considered as signal events for this analysis. They are found in significant numbers in the satellite and 5-prong channels and are counted as signal in this analysis.

A potentially serious problem is the presence of background, where the correlation between the primary quark charge and the charge q tagged by the D candidate is preserved. These events will be asymmetric in $q\cos\theta$, thereby introducing an asymmetry into the background. Such correlations are possible e.g. by enriching the sample with true kaons, or with true leptons. These events are present at low levels in all modes considered, and need to be taken into account properly.

The level of background is determined using different techniques in the D^{*+} and the D^0, D^+ meson decays. In the D^{*+} decay modes a hemisphere mixing technique is employed [2], whereby the candidate track for the slow pion is taken from the opposite hemisphere, after being reflected through the origin. No requirements are made on the charge of the D^0 candidate tracks, except, that the total charge of all tracks including the slow pion candidate should be ± 1. Monte Carlo studies have shown that this estimator models the shape of the background very well in all five channels.

The background is determined by normalising the estimator distribution for $0.18 < \Delta M < 0.20$ ($0.19 < \Delta M < 0.22$ for the semileptonic channels) to the sideband of the signal distribution and subtracting the normalised background from the signal. Candidates are counted within the ΔM ranges given in tables 1. Monte Carlo studies have shown that this method leads to an unbiased determination of the number of D^{*+} candidates in all channels.

In the D^0 and D^+ channels a fit is performed to the observed mass spectra with a phenomenologically determined functional form for the background. The background to the D^0 is described by a polynomial of third degree, while in the D^+ an exponential folded with a gaussian function is used. Contributions from satellite decays visible in the D^0 mass spectrum at masses around 1.6 GeV, are accounted for by an additional gaussian function. A slight asymmetry in the peak is allowed for by fitting different widths below and above the mean value. The normalisation, mean and both widths are determined in the fit.

In both channels background exists which will distort the expected signal shape. In the D^0 channel, the decays $D^0 \to K^+K^-$ and $D^0 \to \pi^+\pi^-$ contribute to the signal, where one of the final state particles is misreconstructed as either a pion or a kaon, thus faking a $K\pi$ final state. Since the charge correlation between the primary quark and the reconstructed charge is broken, their estimated contribution is subtracted from the sample. Simulated events are used to estimate the contribution from these two sources and it is found to contribute less than 1% to the final sample. The same background is present in the 3-prong D^{*+} channel, though at an even lower level. Its contribution has been estimated in [3] and is subtracted from the sample.

Backgrounds in the D^+ reconstruction are the decays of the D_s meson into $\phi\pi^+$ and $K^{*0}K^+$, both decaying into a final state $K^+K^-\pi^+$. Misidentifying a kaon as a pion will shift the mass peak to around the mass of the D^+ meson. Since the charge correlation to the primary quark is conserved for a large fraction of these decays, they have to be treated carefully. Monte Carlo studies have shown that they contribute approximately 10% to the D^+ signal.

The total background in the sample is determined by integrating the fit function over the appropriate mass window, and correcting for the discussed background sources. The number of signal candidates is obtained by subtracting the number of background events from the total

	$D^{*+} \to D^0\pi$ $\hookrightarrow K\pi$		$D^{*+} \to D^0\pi$ $\hookrightarrow K\pi\pi^0$		$D^{*+} \to D^0\pi$ $\hookrightarrow K\pi\pi\pi$	
x_D	N^{obs}_{cand}	N^{est}_{bck}	N^{obs}_{cand}	N^{est}_{bck}	N^{obs}_{cand}	N^{est}_{bck}
0.2-0.3	2441	1366±34	8296	6163± 79		
0.3-0.4	1486	568 ±22	4151	2418± 49		
0.4-0.5	1006	223 ±14	2453	1026± 32		
0.5-0.6	1277	322 ±15	3006	1411± 36	4423	2688± 47
0.6-0.7	733	132 ± 9	1377	567 ± 22	1752	826 ± 25
0.7-0.8	417	58 ± 6	542	218 ± 13	718	242 ± 12
0.8-1.0	230	31 ± 4	164	74 ± 7	294	63 ± 5

	$D^{*+} \to D^0\pi$ $\hookrightarrow K\ell\nu$		$D^0 \to K\pi$		$D^+ \to K\pi\pi$	
x_D	N^{obs}_{cand}	N^{est}_{bck}	N^{obs}_{cand}	N^{est}_{bck}	N^{obs}_{cand}	N^{est}_{bck}
0.2-0.3	1907	977 ±32				
0.3-0.4	1146	396 ±20	3414	2232± 47	5190	4345± 66
0.4-0.5	694	163 ±13	2098	1386± 37	3309	2429± 49
0.5-0.6	713	190 ±13	1411	620 ± 25	1906	1208± 35
0.6-0.7			807	374 ± 19	1054	546 ± 23
0.7-0.8	475	95 ± 9	433	184 ± 14	555	195 ± 14
0.8-1.0			178	66 ± 8	221	54 ± 7

Table 4: Number of D mesons reconstructed in the different decay modes, in bins of the effective scaled energy of the candidates calculated from the reconstructed track momenta. Given are the number of D meson candidates and the number of background events. The error quoted on the estimated background is the statistical error only. Note that in the analysis, signal and background determination is done separately for three classes of events depending on the track reconstruction quality.

number of events in the mass window. This method has been tested using simulated events and has been found to reproduce the true number of D mesons within the statistical errors.

In table 4 the number of D meson candidates in the different channels and the background are listed along with statistical errors. In this sample a total of 19484 ± 137 D^{*+} mesons and 6937 ± 118 D mesons after background subtraction have been reconstructed, over a background of 20217 ± 137 events and 13639 ± 118 events respectively.

In figures 1 and 2 the invariant mass spectra for all seven reconstructed channels are presented. For D^{*+} decays, the mass difference ΔM between the D^{*+} and the D^0 candidate is shown, while for the D^0 and D^+ channel the invariant mass spectrum is plotted directly. In all channels clear signals are visible.

5 Production of Charmed Mesons in Bottom and Charm Events

Nearly all D mesons are produced in bottom and charm decays. An analysis attempting to study properties of the charm quark therefore has to separate the components. Techniques for this have been developed and are applied to the tagged sample. In this section the method of flavour separation is reviewed. In a first step the bottom and charm fractions in the tagged sample are determined. These overall fractions are combined with lifetime information and are used as input for the calculation of event probabilities. This is described in the second part of this section. These event based probabilities will be used in the asymmetry fit.

5.1 Statistical Flavour Separation

The flavour separation technique adopted determines the size of the bottom component in the sample. It depends on the assumption that all D mesons are produced in either charm or bottom decays, and that other flavours contribute exclusively to the background sample. The flavour composition of the D meson sample therefore is determined by measuring the bottom fraction in the sample, after background subtraction. Background subtraction is performed using a sample selected such that its flavour composition describes well the true background.

A small fraction of D mesons can also be produced from the splitting of a gluon into a pair of charm quarks. This process is present in all five flavours. The fraction has been measured in ref. [3,15], and the combined result is used to estimate the systematic errors due to this source.

5.1.1 Bottom Tagging Techniques

Two different bottom tagging techniques are used to determine the flavour composition. The first uses the shapes of jets, which are expected to be significantly different for bottom jets than they are for charm jets. The shapes are measured by a set of seven jet shape variables, containing combinations of the momenta, both transverse and longitudinal components, of the particles in the jets. These variables are used as input to an artificial neural network, which has been trained using data and Monte Carlo for b/c separation. A detailed description of the variables and the method may be found in ref. [3,16]. A similar procedure has been used by the ALEPH collaboration in ref. [17]. The network was developed for the analysis of D^{*+} decays and is applied to the D^{*+} sample in this work.

In the second method hadronic decays of the Z^0 into bottom quarks are tagged by taking advantage of the relatively long lifetimes of bottom flavoured hadrons compared to lighter flavour ones. For each jet in the event, a secondary vertex is reconstructed by an iterative procedure. In a first step all tracks which pass the quality requirements are used to form a common vertex. Tracks are removed from the vertex fit if they contribute more than 4 to the χ^2 of the fit. This is continued until either no track contributes more than 4 to the χ^2, or until less than four tracks remain, in which case the vertex finder fails for this jet. A decay length is calculated between this vertex and the primary vertex in the event, constrained to the direction of the jet in which the vertex was found. This is determined in the plane perpendicular to the beam direction. Finally, the significance for this distance is calculated and used for the b-tag. A very similar procedure has been used in [18].

The decay length significance and the neural network output are calculated for the jet not containing the D candidate. If more than two jets are found in the event the jet with the highest energy not containing the D meson candidate is chosen. This requirement enriches the sample in jets originating from a primary quark as opposed to gluons.

In the D^{*+} 3-prong, D^0 and D^+ channels the decay length significance distribution is also determined in the jet containing the D candidate, similar to the procedure developed in [3].

5.1.2 Treatment of the Background

The treatment of the background is crucial to the success of the flavour separation method. The measurement of the charm fraction by subtracting the bottom fraction in the sample is only justified if the distributions of the tagging variable for background events are known.

The samples used to estimate the behaviour of the background in the tagging variables are selected using the background estimation techniques discussed in connection with the determination of the number of candidates.

The background sample used in the lifetime analysis in the D^{*+} channels is selected by requiring a reflected pion D^{*+} candidate in one jet, and using the highest energy jet not containing the candidate to calculate the lifetime significance of the background candidate event. Candidates are searched for over an extended range of ΔM as indicated in table 5.

The background sample used in the neural net analysis is based upon a wrong charge technique, where a D^0 candidate is reconstructed with an unphysical charge of two (e.g. a $K^+\pi^+$ for the 3-prong channel) by combining tracks appropriately. This is done in a sideband in the ΔM distribution. The sidebands chosen are given in table 5.

The decay length significance background distributions in the D^0 and D^+ channels are selected in sidebands of M_D, above (for the D^0 and the D^+) and below (for the D^+) the mass of the expected signal. The region below the D^0 mass can not be used since the decay $D^0 \to K\pi\pi^0$ contributes there. Details of the selection of the samples are given in table 5.

Monte Carlo studies show that the decay length significance and neural net output distributions expected for true backgrounds are well reproduced by the distributions obtained in the background tagged samples.

5.1.3 Determination of the Charm Fraction

To obtain the charm fraction in each sample, the number of bottom tagged events is determined. The number, N_{b-tag}, of events exceeding a particular decay length significance or some value of the neural net output in a sample of N_{cand} events, is given by:

$$\frac{N_{b-tag}}{N_{cand}} = (1 - f_{bgd}) \cdot [f_b \cdot \mathcal{P}_b + f_c \cdot \mathcal{P}_c] + f_{bgd} \cdot \mathcal{P}_{bgd} \ , \qquad (4)$$

where f_{bgd}, f_b and $f_c = 1 - f_b$ are the fractions of background, bottom and charm in the sample, and $\mathcal{P}_{bgd,b,c}$ describe the probabilities that the D meson from this source is tagged. Assuming that the tagging probabilities $\mathcal{P}$ are known, and that the background fraction has been measured, the bottom and thereby the charm fraction f_c can be determined. This method is the same as used in ref [3], where additional details may be found.

channel	variable	decay length significance range	decay length significance estimator	neural network range	neural network estimator
3-prong, satellite, 5-prong	ΔM	$0.140 - 0.200$	R	$0.180 - 0.200$	Q
lepton	ΔM	$0.140 - 0.220$	R	$0.190 - 0.220$	Q
D^0	M_{D^0}	$1.95 - 2.50$	S	-	-
D^+	M_{D^+}	$1.75 - 1.81, 1.93 - 1.99$	S	-	-

Table 5: Different background estimators used in the six D meson channels. Shown is the variable, in which the background is selected, the range over which events are accepted, and the type of estimator used. For the latter S corresponds to the correct charge selection, done in the mass range indicated, Q to the wrong charge one, and R to the reflected pion sample. Estimators are listed for the decay length significance and the neural network analysis. A more detailed discussion of the background and their application can be found in the text.

The probabilities $\mathcal{P}$ are calculated as far as possible from data. Distributions of the tagging variables are produced in the data for both signal and background candidates. The decay length distribution for background subtracted D meson candidates is shown in figure 3(a). Superimposed is the prediction from Monte Carlo simulation of the same variable. In figure 3(b) the neural network output variable is shown for the D^{*+} candidates after background subtraction.

Bottom events are tagged by requiring large decay length significances ($d/\sigma > 8$) or neural network outputs close to one. For the jet shape analysis, the tagging probabilities $\mathcal{P}_b$ that a b-event results in a particular network output have been calculated in [3] from data, using events enriched in bottom by the presence of a high momentum lepton. The tagging probability $\mathcal{P}_c$ for the jet shape analysis has been determined from the simulation. For the decay length significance Monte Carlo simulation has been used to calculate the expected distributions from both charm and bottom events. The total number of b events is obtained using eq. 4.

The analysis is repeated for looser cuts on the decay length significance of $6, 4$ and 2. For the jetshape analysis the output distribution has been subdivided into four roughly equally populated regions, and the separation is repeated for each of the regions. The different results are combined taking the correlations between the samples into account. The analysis is performed separately in all channels, and for each bin of x_D, as defined in table 4.

The final results of this analysis are the charm fractions $f_c(x_D)_{channel}$ as a function of the scaled energy for each channel separately. In table 6 the charm fractions are given combined into two bins of x_D, for each channel. The systematic errors shown in the table will be discussed in detail later in this note.

5.2 Event Probabilities

The charm fractions determined for an ensemble of candidates are extended into event-by-event weights using decay length significance information calculated in the highest energy jet not containing the D candidate. The jet containing the D meson candidate is not used because

channel	$0.2 < x_D < 0.5$ $f_c \pm \sigma_{stat} \pm \sigma_{sys}$	$x_D > 0.5$ $f_c \pm \sigma_{stat} \pm \sigma_{sys}$
3-prong	0.325±0.024±0.048	0.844±0.020±0.025
satellite	0.435±0.030±0.011	0.855±0.027±0.045
5-prong	–	0.806±0.029±0.083
electron	0.433±0.051±0.051	0.948±0.046±0.035
muon	0.507±0.047±0.048	0.908±0.045±0.032
	$0.3 < x_D < 0.5$	$x_D > 0.5$
D^0	0.336±0.067±0.099	0.769±0.065±0.108
D^+	0.407±0.119±0.130	0.788±0.080±0.077

Table 6: List of charm fractions in the different channels with their statistical and systematic errors. Results both for $0.2 < x_D < 0.5$ and $x_D > 0.5$ are shown to illustrate the increasing charm purity with increasing x_D. Note that the x_D used is the one calculated from the observed tracks, and the same $x_{\rm D}$ could correspond to a different true scaled energy of the D meson in different channels.

lifetime information in this jet is sensitive to the time dependent mixing in the B system. The measurement of the decay length significance, $d/\sigma \equiv \delta$, in a specific event is compared to the expected distributions for signal, background, bottom and charm events, and a probability for this measurement is calculated.

As far as possible data are used to calculate the probabilities. The distributions for all candidates, L_{cand}, and for background events, L_{bgd} are taken directly from measurements. The background distributions are estimated from events tagged using candidates in a sideband in ΔM, $M_{\rm D^0}$ or $M_{\rm D^+}$, with mass cuts as given in table 5. Using the number of signal and background events given in table 4 the weights for an event being a signal or a background event can be calculated:

$$\begin{aligned} w_{sig}(x_i,\delta_i) &= L_{cand}(x_i,\delta_i) - f_{\rm bgd}(x_i)\cdot L_{\rm bgd}(x_i,\delta_i) \\ w_{bgd}(x_i,\delta_i) &= f_{\rm bgd}(x_i)\cdot L_{bgd}(x_i,\delta_i) \end{aligned} \qquad (5)$$

The functions $L(x_i,\delta_i)$ are the probability density functions of the decay length significances. The fractions $f_{\rm bgd}(x) = N_i^{\rm bgd}(x)/N_i^{cand}(x)$ are calculated in bins of x, as described above, and separately in each channel, from the number given in table 4.

Monte Carlo simulation is used to predict the equivalent distributions for bottom and charm even , $L_{\rm c}(\delta)$ and $L_{\rm b}(\delta)$. The weights are given by:

$$\begin{aligned} w_{\rm b}(x_i,\delta_i) &= \frac{f_{\rm b}(x_i)L_{\rm b}(x_i,\delta_i)}{f_{\rm b}(x_i)L_{\rm b}(x_i,\delta_i) + f_{\rm c}(x_i)L_{\rm c}(x_i,\delta_i)} \\ w_{\rm c}(x_i,\delta_i) &= \frac{f_{\rm c}(x_i)L_{\rm c}(\delta_i)}{f_{\rm b}(x_i)L_{\rm b}(x_i,\delta_i) + f_{\rm c}(x_i)L_{\rm c}(x_i,\delta_i)} \ . \end{aligned} \qquad (6)$$

Here $f_{\rm b}(x_i), f_{\rm c}(x_i)$ are the fraction of bottom, charm events in the sample, which have been determined on a statistical basis in bins of x, and L are the probability density functions for the decay length significance distribution, for the candidate type indicated.

6 Measurement of the Asymmetries

In this section the measurement of the asymmetries is presented. They are extracted from the data using an unbinned log-likelihood fit. The technique used and the likelihood function will be described in the first part of this section. The results of the previous section, the event-by-event weights for an event to be a bottom, charm or background event, are used as input into this fit. The actual fit and its results are discussed in the last part of this section.

6.1 The Likelihood Function

The forward–backward asymmetry is defined as

$$A_{FB} = \frac{\int_0^1 \frac{d\sigma}{dy} dy - \int_{-1}^0 \frac{d\sigma}{dy} dy}{\int_0^1 \frac{d\sigma}{dy} dy + \int_{-1}^0 \frac{d\sigma}{dy} dy} \tag{7}$$

where y is the cosine of the polar angle of the outgoing fermion with respect to the incoming fermion. In events containing a D meson, the direction y is approximately described by $y = q \cdot \cos(\theta_{thrust})$, where q is the charge of the D and θ_{thrust} is the angle of the thrust axis with respect to the beam. The sign of the thrust axis is chosen such that the scalar product of the thrust axis with the D direction is positive.

The asymmetry is determined in an unbinned log-likelihood fit to the thrust distribution signed by the charge of the D meson candidate. The likelihood function has the form

$$\log \mathcal{L} = \sum_i \log(1 + y_i^2 + \frac{8}{3} \cdot A_{\rm FB}^{\rm obs} \cdot y_i) \; . \tag{8}$$

The sum runs over all candidates i considered.

The total observed asymmetry has contributions from bottom, charm and background events, resulting in a total probability density function

$$\mathcal{L}_i \;\; = \;\; 1 + y_i^2 + \frac{8}{3} \cdot \left[w_{sig} \cdot (w_{\rm b} \cdot (1 - 2\zeta_{\rm D})(1 - 2\chi_{\rm D}) A_{\rm FB}^{\rm b} + w_{\rm c} \cdot A_{\rm FB}^{\rm c}) + w_{bgd} A_{\rm FB}^{\rm bgd} \right] y_i \; . \tag{9}$$

Here $w_{sig,bgd,\rm b,c}$ is the event weight of a D mesons to originate from the source indicated, $\chi_{\rm D}$ is the average time integrated $\rm B^0$–$\overline{\rm B}^0$ mixing in the D sample, and $A_{\rm FB}^{\rm bgd}$ allows for a possible asymmetry in this background. The $\rm B^0$–$\overline{\rm B}^0$ mixing parameter, $\chi_{\rm D}$, is the one appropriate for the sample of D mesons, which originate mostly neutral B mesons and a small fraction of charged B mesons. It is estimated separately for $\rm D^{*+}$, $\rm D^0$ and $\rm D^+$ channels. Differences between the different channels are expected because the production mechanism are somewhat different, and because the lifetime cut applied to the $\rm D^0$ and $\rm D^+$ channel biases the effective mixing in this sample. "Wrongly" charged $\rm D^-$ mesons can be produced in b-decays via the suppressed production of a $\overline{\rm c}$ quark in the decay of a W into $\overline{\rm c}$s. The contribution to the sample from this source is estimated to be less than 1%. This results in a mixing like parameter $\zeta_{\rm D}$, which describes the fraction of D mesons produced with the wrong sign in the full sample. In table 7 the actual values used for the different channels are given.

channel	ζ_D	χ_D^{eff}
D^{*+}	0.025 ± 0.025	0.160 ± 0.019
D^0	0.025 ± 0.025	0.080 ± 0.026
D^+	0.028 ± 0.028	0.176 ± 0.023

Table 7: List of the effective mixing parameter χ_D appropriate for the different channels, and for ζ_D, the fraction of wrong sign D mesons in the sample.

6.2 Background Asymmetry

As discussed above background can present a serious problem if, for a significant fraction of events, a charge correlation exists between the primary quark in the event and the charge tagged by the D meson candidate. Monte Carlo studies show that such correlations exist at a significant level in the different channels. These studies also indicate that the amount of correlation does not depend on ΔM, M_{D^0} or M_{D^+}, allowing it to be measured in sidebands in ΔM and M_{D^0}, M_{D^+} respectively. From the simulation it is found that typical charge correlations are of the order of a few percent in the non-leptonic D channels, and around 10% in the leptonic channels. This translates into expected background asymmetries below 1% in most channels. The Monte Carlo shows that the sideband describes the charge asymmetries to better than 0.1%, with no systematic effects visible. Nevertheless the observed differences between true background and sideband charge asymmetries will be used as systematic errors due to this source.

The fit is extended to determine simultaneously the background asymmetries in the samples by constraining them to their values in the appropriate sidebands. The sidebands used are the same as were used in the estimation of the background distributions, and are summarised in table 5.

6.3 Results of the Fit

The samples collected on, below and above the peak of the Z^0 resonance have been fitted to extract A_{FB}^c and A_{FB}^b. The final probability density function used to construct the likelihood is given by equation 9. The bottom asymmetry, the charm asymmetry and the background asymmetries are free parameters in the fit. The latter one is allowed to vary independently in each on the seven channels considered. It should be noted however that the background asymmetries are essentially determined from the sidebands, and are nearly totally decoupled from the charm and bottom asymmetries.

The results of the fits are

$$\begin{aligned}
A_{FB}^c &= -0.006 \pm 0.068 \quad A_{FB}^b = 0.027 \pm 0.169 \quad \langle E_{cm} \rangle = 89.54 \text{ GeV} \\
A_{FB}^c &= 0.068 \pm 0.014 \quad A_{FB}^b = 0.112 \pm 0.035 \quad \langle E_{cm} \rangle = 91.20 \text{ GeV} \\
A_{FB}^c &= 0.171 \pm 0.058 \quad A_{FB}^b = -0.267 \pm 0.140 \quad \langle E_{cm} \rangle = 92.94 \text{ GeV}
\end{aligned}$$

with a statistical correlation coefficient between the bottom and charm asymmetry of -0.414 (-0.411 and -0.402 for the low and high energy point, respectively). The energies indicated are a luminosity weighted average of the appropriate off peak and on peak points respectively.

The result of the fit is illustrated in figure 4, where the differential asymmetry, $\Delta A_{FB} = (n_F(y) - n_B(y))/(n_F(y) + n_B(y))$ is shown as a function of y, with the result of the fit superimposed. $n_{F,B}(y)$ are the number of candidates in the forward (backward) y hemisphere. The results are plotted as a function of the center of mass energy in figure 5. Also shown is the prediction of the standard model for a top mass of 180 GeVand a Higgs mass of 300 GeV. In figure 6 the correlation between $A_{\rm FB}^{\rm c}$ and $A_{\rm FB}^{\rm b}$ is illustrated, and the predictions of the standard model for the asymmetries on the peak of the $\rm Z^0$ resonance are shown.

The fit has been repeated with the bottom asymmetry set to its standard model expectation of $A_{\rm FB}^{\rm b} = 0.0935$, obtained for a Higgs mass of 300 GeV and a top mass of 180 GeV. The result on the peak of the $\rm Z^0$ resonance is:

$$A_{\rm FB}^{\rm c} = 0.071 \pm 0.013$$

in good agreement with the above two parameter fit.

7 Checks and Systematic Errors

The stability of the fit procedure has been checked by repeating the analysis individually for each of the seven channels, and comparing the results. Consistent results are obtained.

Two groups of systematic errors affect the analysis. The first group is related to errors specific to this analysis and the determination of the asymmetry. The second group concerns errors related to the separation of the sample into its bottom and charm component. This latter error will only be reviewed here rather briefly, since a more detailed discussion may be found in [3].

A number of systematic effects can influence the asymmetry fit results. The following sources have been considered:

- One of the advantages of the likelihood fit is that it is independent of the experimental acceptances. This is only true if the ratio between signal and background acceptances is constant over the different $\cos\theta$ regions for which they have been determined. The influence of this assumption has been investigated by repeating the fit with signal and background determined in only one bin of $\cos\theta$. Possible deviations from this assumption can be caused by the changing mass resolution as a function of $\cos\theta$, which might affect signal and background differently. The effect is found to be small.

- The acceptance in the detector has been studied for signs of possible asymmetries in $q\cos\theta$. No indication of any effect has been found, neither in the simulation nor in the data.

- Heavy flavour production in gluon initiated jets will contribute at a low level to the sample of D mesons tagged. A first measurement of this contribution has been presented in [3, 15], in agreement with current theoretical predictions. The measured rate from gluon splitting, $n_{\rm g\to c\bar{c}} = 2.38 \pm 0.48\%$, has been subtracted from the tagged sample, with 50% of the contribution assigned as a systematic error from this source.

$\langle E_{cm} \rangle$	89.54 GeV		91.20 GeV		92.94 GeV	
Systematic error source	$\Delta(A_{FB}^c)$	$\Delta(A_{FB}^b)$	$\Delta(A_{FB}^c)$	$\Delta(A_{FB}^b)$	$\Delta(A_{FB}^c)$	$\Delta(A_{FB}^b)$
general errors						
same acceptance for background and signal	0.0009	0.0028	0.0009	0.0028	0.0009	0.0028
background level	0.0038	0.0101	0.0014	0.0062	0.0038	0.0113
contribution from $W \to D(\zeta_D)$	-	+0.0014	-	+0.0061	-	−0.0130
effective $B-\overline{B}$ mixing in D events	-	+.0024	-	+0.0096	-	−0.0230
thrust instead of quark direction	0.0010	0.0010	0.0010	0.0010	0.0010	0.0010
$g \to c\overline{c}, b\overline{b}$	+0.0002	−0.0008	+0.0020	0.0034	+0.0050	−0.0078
background asymmetry	0.0010	0.0023	0.0010	0.0023	0.0010	0.0023
x − dependence of background asymmetry	0.0018	0.0051	0.0018	0.0051	0.0018	0.0051
b-c separation related errors						
Monte Carlo statistics	0.0084	0.0248	0.0018	0.0052	0.0094	0.0264
background estimator	0.0039	0.0110	0.0039	0.0110	0.0039	0.0110
charged multiplicity in jets	−0.0036	+0.0218	−0.0023	+0.0022	+0.0046	+0.0183
charm modelling	0.0030	0.0054	0.0030	0.0054	0.0030	0.0054
detector response	0.0007	0.0022	0.0002	0.0005	0.0011	0.0023
detector resolution	0.0022	0.0064	0.0022	0.0005	0.0014	0.0068
Heavy flavour fragmentation	0.0005	0.0015	0.0001	0.0003	0.0007	0.0015
Hemisphere bias	0.0023	0.0039	0.0023	0.0039	0.0023	0.0039
Bottom hadron lifetime	−0.0017	+0.0065	−0.0003	+0.0005	−0.0021	+0.0026
total	0.0120	0.0385	0.0071	0.0205	0.0151	0.0495

Table 8: List of the systematic errors contributing to the measured asymmetries of the processes $e^+e^- \to c\overline{c}$ and $e^+e^- \to b\overline{b}$, for the three ranges of center of mass energy investigated. A sign in front of an error indicates the direction of change under a positive change of the variable.

- The determination of the background asymmetries depends on the assumption, that the sidebands correctly reproduce the charge correlation present in the true background. This assumption has been checked in the simulation. Typical charge correlations are found to be of the order of a few percent, and differences between sideband and true background below 0.1%. The observed differences are used as systematic errors from this source.

- A possible bias in the background asymmetries as a function of x_D has been investigated by splitting the background samples into two bins of x_D, and repeating the fit. The difference has been assigned as the systematic error. Its size is also consistent with Monte Carlo studies.

The errors considered in connection with the flavour separation are:

- Monte Carlo Statistics: The determination of the tagging probabilities relies partially on

Monte Carlo. This error is due to the finite statistics of the Monte Carlo available.

- Background estimators: Some differences may exist between the true background and the background estimators used. They are the source of the largest systematic error. It should be noted however that this error has a large statistical component due to the finite size of the Monte Carlo sample available.
- Heavy flavour multiplicity: The multiplicity for heavy flavour decays in the Monte Carlo has been varied by reweighting simulated events, corresponding to the current experimental bounds.
- Charm modelling: The modelling of the shape of charm jets, of multiplicities and momenta flow in charm jets is another important source of systematic error, introduced by the jetshape analysis. This error also includes effects due to possible differences in the decay length distribution of jets originating from charm quark decays, between data and simulation. This latter part of the error has been calculated by repeating the analysis after determining the charm decay length distribution nearly entirely from data. This is possible, since the decay length significance distribution of the candidates, of background and of bottom jets are known. The observed differences in the asymmetries are used as systematic error.
- Detector response: Non-uniformity of the detector response as a function of $\cos\theta$ gives rise to this error. This error is present for the jetshape analysis.
- Detector resolution: The resolution of the track parameters in the Monte Carlo is varied by $\pm 20\%$.
- Heavy flavour fragmentation: The parameters for the charm and bottom fragmentation function are varied within their experimental limits.
- Hemisphere bias: This errors describes a possible bias between the D-jet and the jet used to calculate the tagging variables used in the flavour separation.
- Bottom hadron lifetime: The B-hadron lifetime has been varied within its current experimental error.

A list of all systematic errors considered is given in table 8.

8 Results and Summary

The forward–backward asymmetries of the processes $e^+e^- \to c\bar{c}$ and $e^+e^- \to b\bar{b}$ have been measured using 27651 ± 247 D^{*+}, D^0 and D^+ candidate events containing 25095 signal events on the peak of the Z^0 resonance, 1127 events below and 1429 above the peak off the resonance. The result of the fit with both the b and the c asymmetry as free parameters is

$$\begin{array}{lll}
A_{\mathrm{FB}}^{\mathrm{c}} = -0.006 \pm 0.068 \pm 0.012 & A_{\mathrm{FB}}^{\mathrm{b}} = 0.027 \pm 0.169 \pm 0.039 & \langle E_{cm} \rangle = 89.54 \text{ GeV} \\
A_{\mathrm{FB}}^{\mathrm{c}} = 0.068 \pm 0.014 \pm 0.007 & A_{\mathrm{FB}}^{\mathrm{b}} = 0.112 \pm 0.035 \pm 0.021 & \langle E_{cm} \rangle = 91.20 \text{ GeV} \\
A_{\mathrm{FB}}^{\mathrm{c}} = 0.171 \pm 0.058 \pm 0.015 & A_{\mathrm{FB}}^{\mathrm{b}} = -0.267 \pm 0.140 \pm 0.050 & \langle E_{cm} \rangle = 92.94 \text{ GeV}
\end{array}$$

in good agreement with the corresponding measurement using high momentum leptons [19] and other measurements at LEP [20].

The fit has been repeated with the bottom asymmetry fixed to its standard model value, resulting in a charm asymmetry measurement of

$$A_{\rm FB}^{\rm c} = 0.071 \pm 0.013 \pm 0.008$$

in good agreement with the above numbers.

Compared to the previous OPAL analysis in ref [2] both the size of the sample has been increased significantly, and the separation between the bottom and the charm components is much improved. As a result in particular the errors of the bottom asymmetries decreased. Comparing the results of the two parameter fit in [2] and this paper, the significances of the differences between the results are $+0.65, -1.24$ and -1.60 σ for the low energy point, on peak point, and the high energy point, respectively, indicating an overall reasonable agreement between both measurement.

The results are consistent with the standard model predictions of $A_{\rm FB}^{\rm c} = 0.061$ and $A_{\rm FB}^{\rm b} = 0.0935$, which were obtained using the program ZFITTER [21] at a centre of mass energy of 91.27 GeV, assuming a top mass of 180 GeV and a Higgs boson mass of 300 GeV. They are also consistent with the predicted energy dependence.

References

[1] For a recent review see e.g. T. Behnke, D.G. Charlton, CERN-PPE/95-11.

[2] OPAL Collaboration, R. Akers *et al.*, Z. Phys. **C 60** (1993) 601.
OPAL Collaboration, *Updated measurement of the Forward-Backward Asymmetry of* $e^+e^- \to b\overline{b}$ *and* $e^+e^- \to c\overline{c}$ *on and near the* Z^0 *peak using* D^{*+} *mesons.* OPAL physics note PN125, March 11, 1994

[3] OPAL Collaboration, R. Akers *et al.*, Z. Phys. **C 67** (1995) 27.

[4] OPAL Collaboration, *A study of* D^0 *and* D^+ *production in* Z^0 *decays.* OPAL physics note PNxxx, submitted to EPS-HEP-95 Brussels, ref. eps 0284

[5] OPAL Collaboration, K. Ahmet *et al.*, Nucl. Instr. Meth. **A 305** (1991) 275;
P.P. Allport *et al.*, Nucl. Instr. Meth. **A 324** (1993) 34;
P.P.Allport *et al.*, Nucl. Instr. Meth. **A 346** (1994) 476;
O. Biebel *et al.*Nucl. Instr. Meth. **A 323** (1992) 169;
M. Hauschild *et al.*, Nucl. Instr. Meth. **A 314** (1992) 74.

[6] OPAL Collaboration, G. Alexander *et al.*, Z. Phys. **C 52** (1991) 175.

[7] JADE Collaboration, W. Bartel *et al.*, Z. Phys. **C 33** (1986) 23;
JADE Collaboration, S. Bethke *et al.*, Phys. Lett **B 213** (1988) 235.

[8] T. Sjöstrand, Comp. Phys. Comm. **39** (1986) 347;
M. Bengtsson and T. Sjöstrand, Comp. Phys. Comm. **43** (1987) 367;
T. Sjöstrand, Int. J. of Mod. Phys. **A 3** (1988) 751.

[9] OPAL Collaboration, M.Z. Akrawy *et al.*, Z. Phys. **C 47** (1990) 505.

[10] C. Peterson *et al.*, Phys. Rev. **D 27** (1983) 105.

[11] The LEP Collaborations, ALEPH, DELPHI, L3 and OPAL, and the LEP Electroweak Working Group, CERN-PPE/94-187, and references therein.

[12] J. Allison *et al.*, Nucl. Instr. Meth. **A 317** (1991) 47.

[13] OPAL Collaboration, R. Akers *et al.*, Phys. Lett. **B 327** (1994) 411.

[14] OPAL Collaboration, R. Akers *et al.*, Z. Phys. **C 60** (1993) 199.

[15] OPAL Collaboration, R. Akers *et al.*, CERN-PPE/95-58.

[16] C.Schwick, *Investigation of the Charm Fragmentation with the OPAL Detector at LEP*, PhD thesis, Hamburg 1994, unpublished.

[17] D. Buskulic *et al.*, Phys. Lett. **B 256** (1991) 218.

[18] OPAL Collab., R. Akers et al., Z. Phys. **C 65** (1995) 17.

[19] OPAL Collaboration, R. Akers *et al.*, Z.Phys. **C 60** (1993) 601;
OPAL Collaboration, R. Akers *et al.*, *Measurement of the Forward-Backward Asymmetries of* $e^+e^- \to b\bar{b}$ *and* $e^+e^- \to c\bar{c}$ *from events tagged by a Lepton, including 1994 data.* OPAL PN 165 (1995); submitted to EPS-HEP-95 Brussels, ref. eps 0279.

[20] DELPHI Collab., P. Abreu et al., Z. Phys. **C 66** (1995) 341.
ALEPH Collaboration, D. Buskulic *et al.*, Phys. Lett. **B 352** (1995) 479.

[21] Calculated using the ZFITTER program described in:
D. Bardin et al., CERN-TH 6443/92 (May 1992); Phys. Lett. B255 (1991) 290; Nucl. Phys. B351 (1991) 1; Z. Phys. C44 (1989) 493.

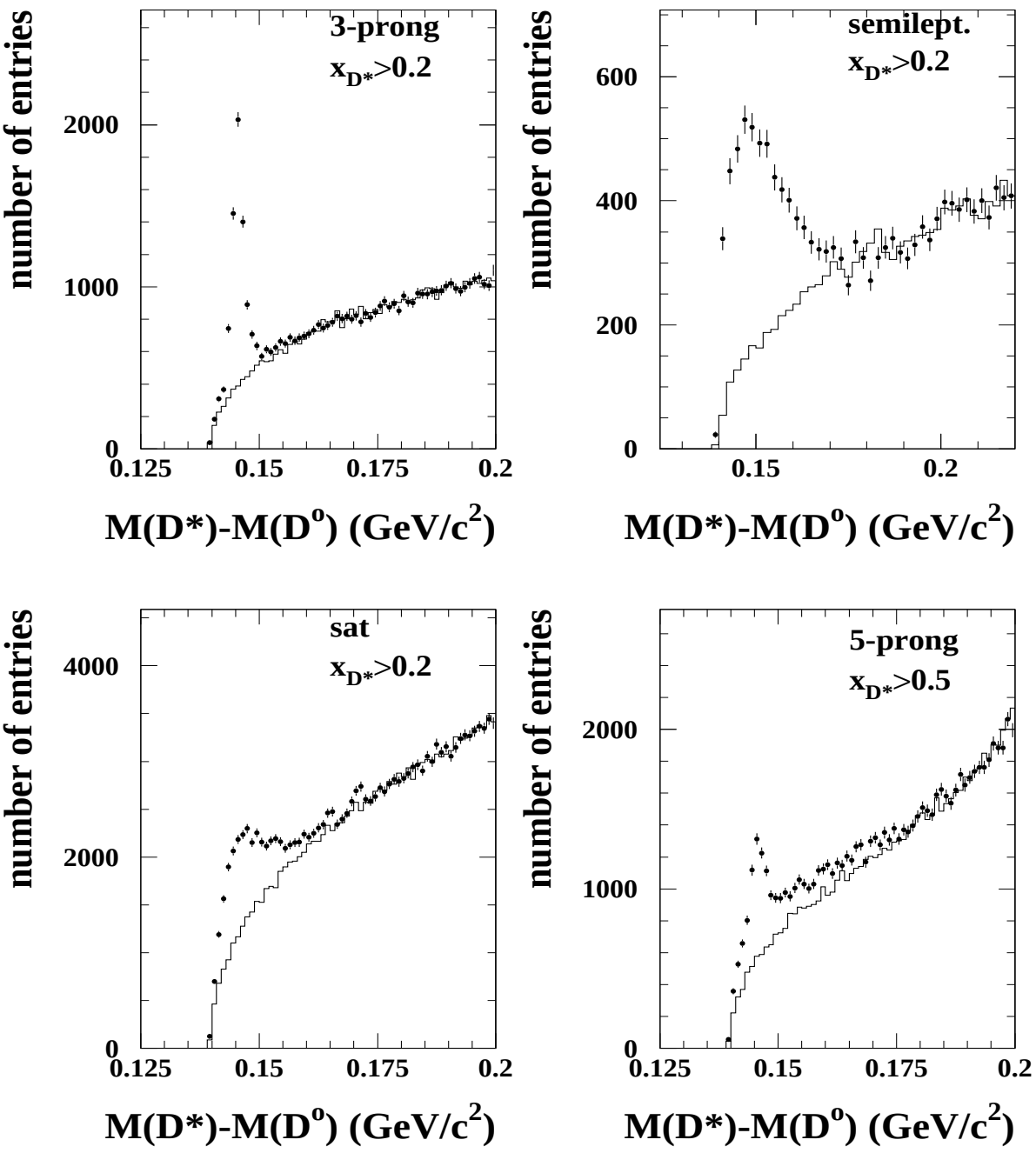

Figure 1: Distributions of the difference $M_{\mathrm{D}^{*+}} - M_{\mathrm{D}^0}$ reconstructed in the four different D^{*+} channels. Both semileptonic decays have been combined into one plot. Superimposed are the background estimator distributions, normalised to the upper sidebands in ΔM.

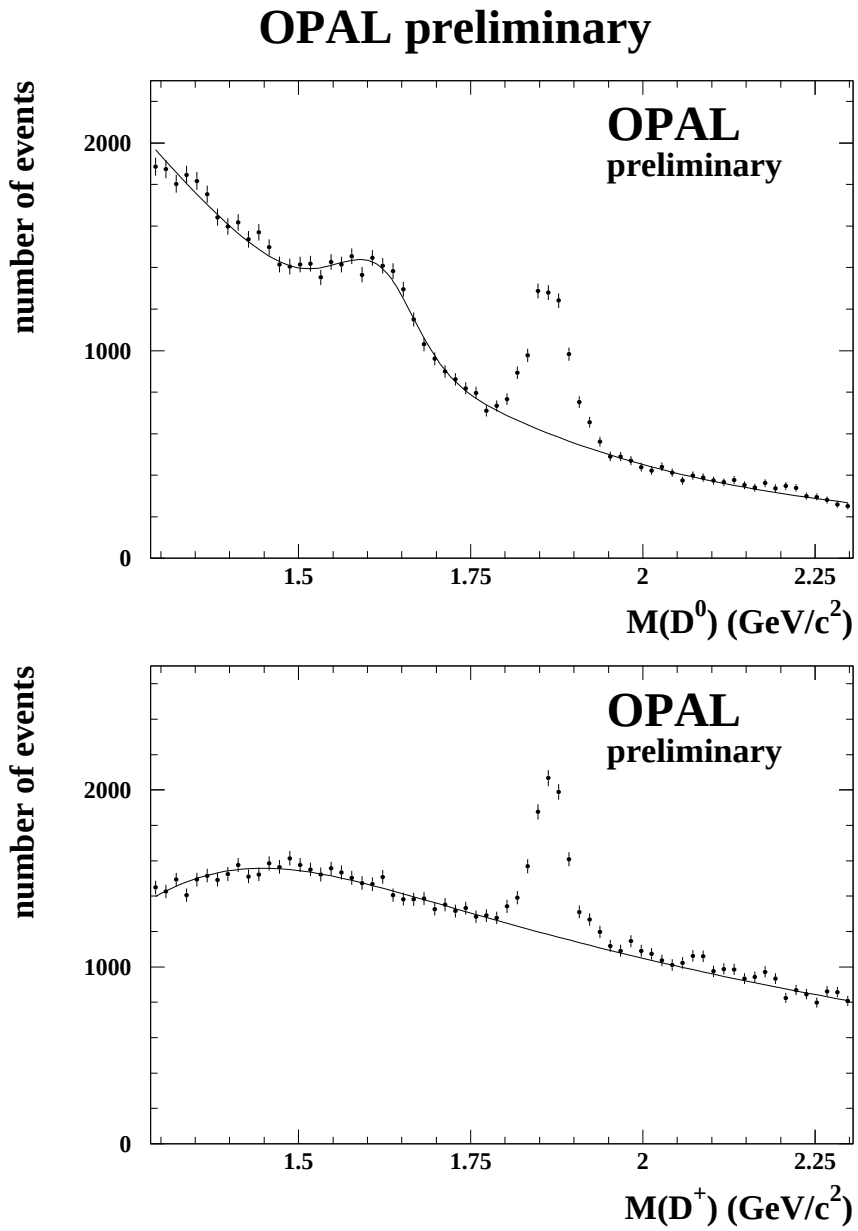

Figure 2: Invariant mass spectra for the D^0 and the D^+ channels. Superimposed is the function used to determine the number of D mesons in each sample.

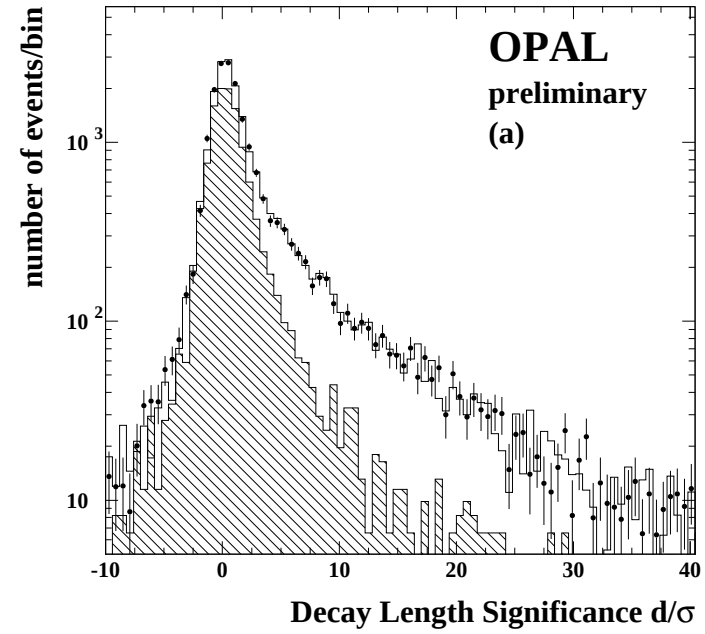

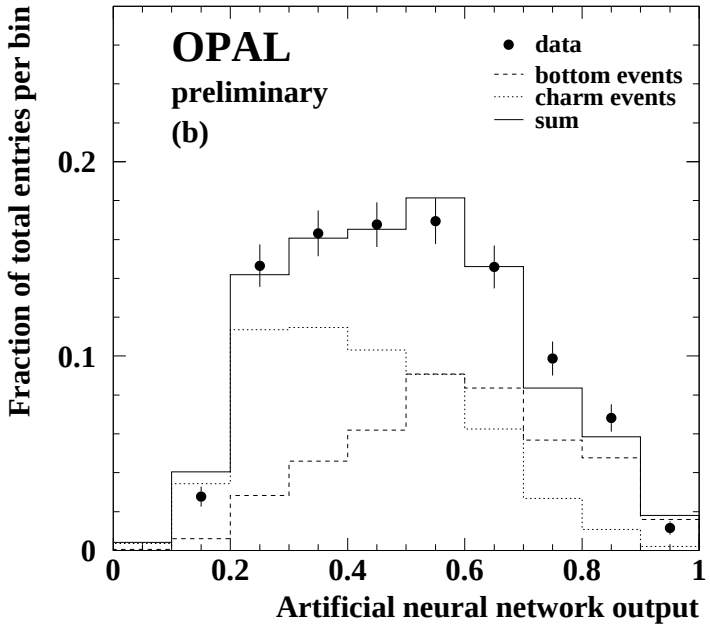

Figure 3: (a) Distribution of the decay length significance in data (points with error bars) and Monte Carlo (line histogram), as reconstructed in the opposite hemisphere from the D^{*+} candidate. The hatched histogram represents the distribution for charm events, as calculated in the simulation, and normalised to the measured charm fraction in the sample. (b) Normalised distribution of the neural network output for D^{*+} candidates (points with error bars), and the expected distribution for $b\overline{b}$ and $c\overline{c}$ events.

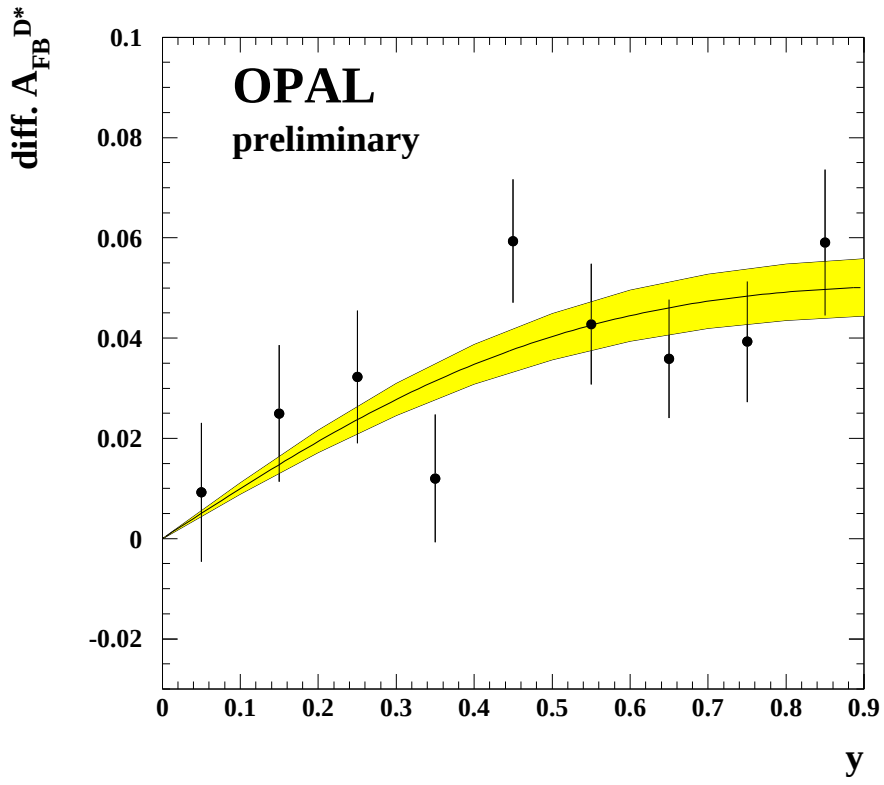

Figure 4: Differential asymmetry as a function of $y = q\cos\theta_{thrust}$, for all candidates, for on peak energies. Superimposed is the result of the fit. The one standard deviation error is indicated by the shaded band.

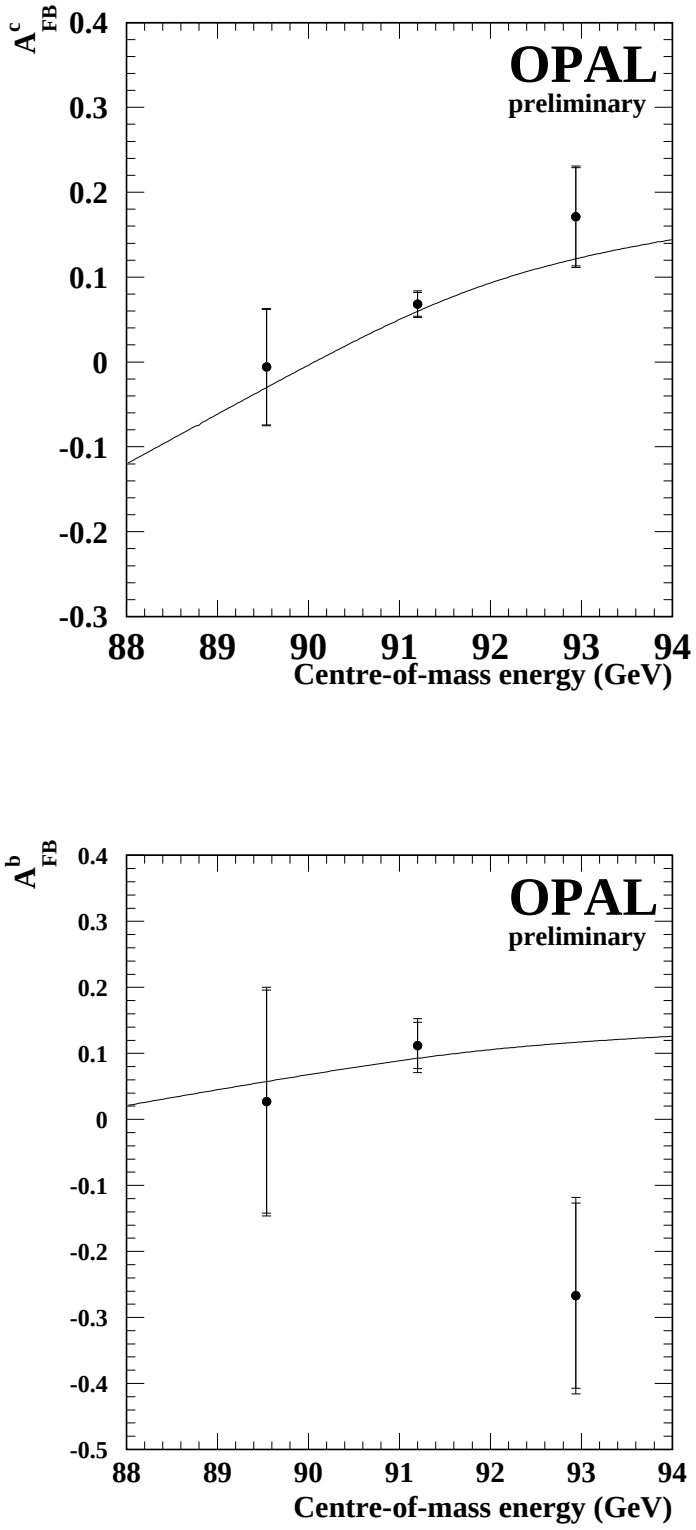

Figure 5: Results for the b and c asymmetries at energies on and around the pole of the Z^0 resonance. The curve shown is the prediction of the standard model for a Higgs mass of 300 GeVand a top mass of 175 GeV. The inner error bars are the statistical errors, the outer one the total error.

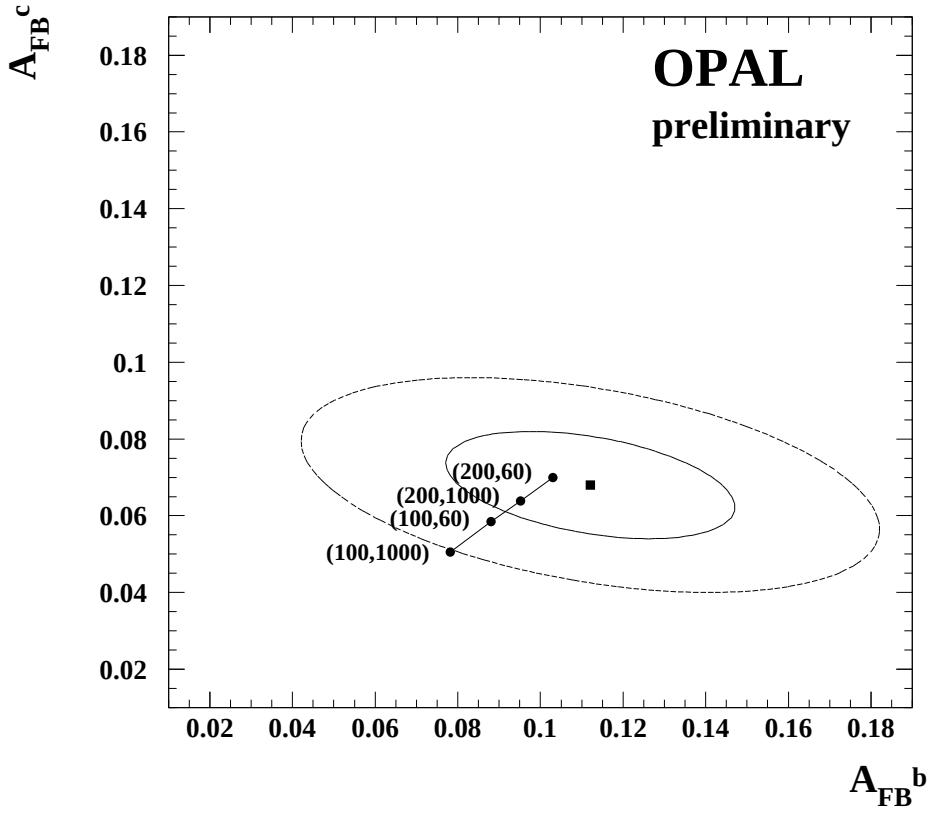

Figure 6: Comparison of the measured b and c asymmetries on the peak of the Z^0 resonance with the standard model prediction for a range of top and higgs masses. The central value is indicated by the square, the contour correspond to 39% and 86% probability, respectively. The line shown illustrates the standard model predictions for the values (m_{top}, m_{higgs}) shown.